Journal of Bio- and Tribo-Corrosion (2024) 10:43
https://doi.org/10.1007/s40735-024-00848-y

# Effect of Varying Cathode–Anode Parameters on Performance of Mild Steel Cathodically Protected by the Aluminum Anode in 0.5 m NaCl Environment

**Daniel Toyin Oloruntoba[1] · Temitope Ebenezer Odemona[1,2] · Olanrewaju Seun Adesina[3,4] · Williams Temitope Owolabi[1] · Olufemi Oluseun Sanyaolu[3,4] · Azeez Lawan Rominiyi[5]**

Received: 19 January 2024 / Revised: 12 April 2024 / Accepted: 16 April 2024


## Abstract

This work investigates the effect of varying cathode–anode parameters on the performance of mild steel cathodically protected by the aluminum anode in 0.5 M NaCl environment. The study aimed to assess the corrosion protection efficacy of the cathodic protection system and identify optimal parameters for maximizing protection while minimizing energy consumption. Impressed current system was employed to drive the aluminum electrons from the anode to the cathode to achieve cathodic protection of the mild steel cathode. Using Optical Electron Microscope, Scanning Electron Microscope with an electron diffraction spectrometer, and X-ray diffraction, the cathodically treated mild steel samples were characterized. The rate of mild steel corrosion was determined by adopting the potentiodynamic polarization method together with the weight loss method in a 0.5 M NaCl environment. Certain parameters including the working voltage, exposure time and electrode separation distance were also used to analyze the optimal features of the cathodic protection during the experiment. The findings demonstrated that, across the distances and exposure times, an aluminum anode operating at working voltages of 3 and 4 V in a 0.5 M NaCl environment provided sacrificial protection for the mild steel (cathode). The working voltage of 4 V yielded the best cathodic protection in 0.5 M NaCl at 5 cm for 15 min. Furthermore, at a working voltage of 5 V, efficient protection of the mild steel was achieved only at electrodes separation distances above 15 cm, while overprotection of the cathode which could possibly cause cathodic disbondment was observed at electrodes separation distances of 5 cm, 10 cm and 15 cm. The results of this experiment have practical implications for the development and improvement of cathodic protection systems for mild steel structures in environments with high levels of chloride. This highlights the significance of considering cathode–anode parameters to effectively reduce corrosion and ensure the long-term structural stability in the maritime industry and sub-sea operations.

**Keywords** Corrosion · Impressed current · Cathodic protection · Weight loss · Mild steel · Aluminum anode

✉ Olanrewaju Seun Adesina
osaadesina@yahoo.com

[1] Department of Metallurgical and Materials Engineering, Federal University of Technology, P.M.B. 704, Akure, Ondo, Nigeria

[2] Department of Chemistry, University of Missouri, Columbia, MO, USA

[3] Department of Mechanical Engineering, Redeemer's University, Ede, Nigeria

[4] SDG 9, Industry, Innovation and Infrastructure, Redeemer's University, Ede, Nigeria

[5] Department of Mechanical and Industrial Engineering, University of Johannesburg, Doornfontein Campus, Johannesburg 2028, South Africa

## 1 Introduction

Carbon steel is one of the most frequently utilized materials in wide range of engineering applications due to its affordability, remarkable mechanical qualities, and exceptional weldability [1, 2]. These applications range from building construction, oil and gas pipes, sea structures, and automotives. According to previous research, normalized carbon steel possesses tensile strength of 350–850 N/mm$^2$ [3]. However, one major challenge of using carbon steel for engineering applications is its poor corrosion resistance properties [4]. Corrosion in carbon steel refers to the degradation, resulting from chemical interactions with its surrounding environment. Carbon steel, a composite material consisting

Published online: 04 May 2024

of iron and carbon, exhibits a susceptibility to corrosion, which is initiated by the interaction between iron and oxygen and water. The initiation of this process occurs when iron, exposed to oxygen and moisture, undergoes oxidation, leading to the development of iron oxide compounds, which are generally referred to as rust. Rust on carbon steel is the most prevalent manifestation of corrosion while the majority of corrosion occurrences are electrochemically inclined, and it includes at least two reactions on the corroding metal surface, known as the oxidation and reduction reactions [5]. At anodic sites, iron (Fe) atoms lose electrons and oxidize into $Fe^{+}$ ions, while at cathodic sites, oxygen and water molecules combine with electrons to form hydroxide ($OH^{-}$) ions [6, 7]. The resulting reaction yields hydrated iron (III) oxide, or rust. Rust is porous and prone to flaking, exposing fresh metal surfaces to further corrosion, perpetuating the cycle until significant weakening or consumption of the metal occurs. Several factors influence the corrosion rate of carbon steel, including exposure to moisture, oxygen concentration, temperature, acidity or pH of the environment, and the presence of corrosive agents like chloride ions. Various types of corrosion can affect carbon steel, including uniform corrosion, pitting corrosion, galvanic corrosion, and crevice corrosion. To mitigate this corrosion occurrence in carbon steel materials, numerous efforts have been undertaken to enhance carbon steel's ability to withstand corrosion such as coatings, galvanization, alloying, cathodic protection, and design considerations. In light of this, Angst et al. [8] in their study on the cathodic protection of soil buried steel pipelines concluded that the key approaches to mitigate corrosion of underground pipelines are cathodic protection and coatings. For corrosion mitigation, two chemical reactions occur. The first reaction occurs primarily to stop an electrical interaction with an electrolyte, while the latter is an electrical form of corrosion prevention on materials which are subjected to the electrolytes [88]. Similarly, Liu et al. [9] in their novel study used reinforced steel rebars produced by chloride in solutions in simulated concrete pores, increased the corrosion resistance using ginger extracts as a greener inhibitor.

It has been proved by various studies that two major types of cathodic protection systems exist. According to Wilson et al. [10], the first system adopts currents generated when two metals or alloys that differ electrochemically are connected metallically and exposed to the electrolyte; this is usually referred to as a sacrificial anode protection system. The second cathodic protection system technique, called an impressed current cathodic protection system (ICCP), uses supplemental anodes and a direct current power source. Sacrificial anode cathodic protection system is widely known to protect oil pipelines, marine, and some domestic structures from corrosion [11]. The dissolving rate and phosphate removal efficiency of higher magnesium might result from applying a current slightly over the pitting potential, which would also enhance the film-free area and accelerate the anodic and cathodic chemical reaction [12]. However, the performance and safety of cathodic protection systems for structures exposed to seawater depend critically on the electrochemical activity of sacrificial anode materials. For instance, Ding et al. [13] in their study on the electrochemical performance of sacrificial anode interfered by DC stray current concluded that the performance of sacrificial anode increases with an increasing chloride ion concentration. In the case of carbon steel, to mitigate the detrimental effects of corrosion, steel components are predominantly safeguarded through the application of sacrificial coatings [14]. Cadmium has been employed as a sacrificial metallic coating in the aerospace, maritime, oil and gas sector for several decades, primarily owing to its exceptional resistance to chloride-containing conditions [15]. The application of electroplated cadmium coatings is commonly accomplished by the utilization of cyanide or sulphate solutions. Regrettably, in the process of electroplating, a portion of the hydrogen undergoes diffusion into the steel, leading to the occurrence of hydrogen embrittlement [16, 17]. Although the absorption of hydrogen by steel poses a potential issue, it is possible to fully release this absorbed hydrogen through a heating process in a furnace, hence preserving the mechanical qualities [18]. Nevertheless, the utilization of cadmium and related derivatives in industrial engineering applications has been linked to detrimental environmental and health consequences. Therefore, it is imperative to replace electroplated cadmium on a global scale [19, 20]. In view of this, Aluminum (Al), Zinc (Zn), and Magnesium (Mg) are typical metals often used for the sacrificial cathodic protection of other metals especially carbon steel [21].

In vital industries like aviation, automotive and maritime industries, aluminum alloys have been employed as a unique material for the manufacture of essential parts for structural purposes owing to their notable strength-to-weight ratios [22]. Furthermore, their low cost and high current capacity make them appealing as anodes for cathodic protection of carbon steel in corrosive environment [23]. Aluminum alloys (Al-alloys) have been proven to be the preferred sacrificial anodes for monitoring and resisting corrosion over magnesium-based sacrificial anodes because of their comparatively low performance. Also, in deep-water exploration, Aluminum anodes (Al-anodes) are also preferred for the cathodic protection of offshore structures over zinc (Zn) anodes because they are lighter and less costly [11]. Additionally, Feng et al. [24] noted that in a seawater environment, Al-anodes showed superior efficacy as a sacrificial anode for mild steel. An inherent drawback of using aluminum as a sacrificial anode is its propensity to develop a highly stable and inert oxide layer. This layer effectively impedes the corrosion of the metal and causes a change in the metal potential towards less-active values [11]. Also, according to Schuman [25], aluminum has

the ability to self-passivate by developing a protective oxide layer, which could lead to a decrease in both its current and potential output. As such, there are very few applications for pure aluminum (Al) as an anode material. To arrive at the most economical design for sacrificial anodic protection, it is important to analyze the efficiency of the Al-anodes. Several research have been conducted to increase the performance of aluminum anodes (Al-anodes) by alloying with other elements to facilitate the de-passivation (oxide film breakdown) and/or shift the operating potential of the metal to a direction that is more electronegative [15, 26].

The possible Al-"X" alloys required to prevent Al passivation and to effectively protect steel cathodically were examined by Silva Campos et al. [15]. Initially, Campos and his team examined "X" as different elements that can be alloyed with Al which included Ag, Bi, Ca, Cr, Cu, Ga, Gd, In, Mg, Mn, Ni, Sb, Si, Sn, V, Ti, Zn, and Zr to test the binary systems' sacrificial properties. A thorough analysis of these elements alloyed with Al was carried out to examine their corrosion characteristics, including their galvanic coupling to steel, in a NaCl electrolyte. Appropriate heat treatments were applied for each of the systems to minimize the impact of the secondary phases on the corrosion properties. Finally, based on their comparative analysis results, the authors [15] suggested Al–5Zn alloys as the most efficient sacrificial Al-based alloys. Umoru [27] also studied the impact of Tin (Sn) composition as a sacrificial anode for Al–Zn–Mg alloy in seawater. The influence of Sn on the Al alloy-anode efficiency was examined. Their findings indicated that the output of the anode consisting of Al–Zn–Mg–Sn alloy displayed a microstructure with enhanced distribution of tin globules and a degradation of passive alumina film network on the surfaces of the anodes. Furthermore, Alzwghaibi et al. [28] carried out a study on the cathodic protection of oil pipelines on aluminum alloys. Their study focused on creating a material that would aid in preventing corrosion of oil pipelines where soil is abundant with streams of seawater. The authors alloyed different percentages of Zn and Mg with the aluminum and reported that all produced Al-alloys provide viable protection for steel pipelines because they give a lesser current density of about 1.51–12.56 μA/cm$^3$. Presently, there is still very limited research work that examines the impact of cathode–anode parameters on the corrosion performance of mild steel in seawater that are cathodically protected by anodes based on aluminum. Hence, the aim of this research work is to investigate the effect of varying cathode–anode parameters (which includes cathode ratio, varying voltages, time and distances) on the performance of mild steel samples, cathodically protected by the aluminum anode in 0.5 M NaCl (which can be compared to seawater) environment. Additionally, in this study, the comparison between weight loss method and potentiodynamic method of determining corrosion rate for cathodic protection was carried out, as well as the influence of varying voltages and time on the cathodic protection of mild steel by Al-anode in 0.5 M NaCl are reported.

## 2 Materials and Methods

### 2.1 Materials

The materials used in this study include,

i. Rectangular-shaped Mild steel sample [sourced from Nigerian Foundry Limited, Lagos, Nigeria and further characterized in the corrosion laboratory, Federal University of Technology Akure]. The shape was selected because they offer a large surface area for interaction with the electrolyte solution, facilitating efficient electrochemical reactions.
ii. Aluminum anodes [sourced from Nigerian Foundry Limited, Lagos, Nigeria and further characterized in the corrosion laboratory, Federal University of Technology Akure].
iii. NaCl solution and distilled water [Sourced from the department of chemistry, Federal University of Technology Akure].
iv. Insulation wires and graphite electrodes (to suspend the mild steel during the weight loss experiment)
v. Copper wire and connecting rods [Sourced from the department of metallurgical and materials engineering, Federal University of Technology Akure].
vi. Epoxy resin, hardener, and catalyst (to aid the mounting of the steel mild samples). [Also sourced from the chemistry department].

The carbon equivalent (CEQ) of the mild used in this work is 0.249. The chemical composition of the mild steel and aluminum used in this work are presented in Tables 1 and 2, respectively.

### 2.2 Equipment

The equipment used for this study is presented in Table 3.

**Table 1** Chemical composition of mild steel

| Element | Fe | C | Mn | Cr | Cu | Si | Ni | P | S | Co | Sn | Others |
|---|---|---|---|---|---|---|---|---|---|---|---|---|
| Composition (wt%) | 98.7 | 0.11 | 0.364 | 0.256 | 0.196 | 0.0981 | 0.095 | 0.041 | 0.043 | 0.010 | 0.018 | Bal |

**Table 2** Chemical composition of an aluminum anode

| Element | Al | Zn | Si | Fe | Mg | Cu | Ti | Others |
|---|---|---|---|---|---|---|---|---|
| Composition (wt%) | 97.5 | 1.5 | 0.368 | 0.326 | 0.11 | 0.016 | 0.02 | Bal |

## 2.3 Methodology

### 2.3.1 Preparation of Working Electrodes

In this study, six mild steel samples of cross-sectional areas 9.9 $cm^2$, 9.54 $cm^2$, 9.61 $cm^2$, 9.72 $cm^2$, 9.75 $cm^2$ and 10.26 $cm^2$, respectively, were selected, and six corresponding aluminum samples of cross-sectional areas 10.41 $cm^2$, 11.48 $cm^2$, 11.56 $cm^2$, 12.55 $cm^2$, 10.55 $cm^2$ and 15.82 $cm^2$ were used for the cathodic protection of the mild steel samples. Each mild steel sample was attached to a copper wire with the aid of an aluminum foil and carefully mounted using epoxy resin, hardener, and catalyst while the other flat surface is left exposed to study the corrosion features and pattern. The exposed metal surface was then smoothened with different grades of emery paper of grit sizes 60, 320, 400, 600 and 1200. The samples were finally sandblasted to a mirror-like surface to enhance surface preparation, adhesion and improve reactivity. The sandblasting was followed by cleaning with acetone, and then finally kept in a desiccator for 24 h to dry effectively. These coupons made of mild steel served as the corrosion's working electrodes. The aluminum samples were used for the cathodic protection procedure of mild steel samples. A hole was also drilled in the middle of the mild steel and aluminum samples to aid the connection of the connecting wires to further enhance passage of current when the samples are fully immersed into the NaCl environment. It is important to note that this experiment was carried out three times to ensure effectiveness, homogeneity, and authenticity of the results.

### 2.3.2 Cathodic Protection System

In this study, both the mild steel and the aluminum were used as the cathode and the anode, respectively. To move the aluminum electrons from the anode to the cathode in this system, the anode was connected to an impressed current system through the copper wires which transport electrons to the cathode. Copper was selected for this because it possesses excellent electrical conductivity and is easy to access. The two arms of the rectifier which comprised of the cathodic and anodic arms were attached in parallel to a connecting rod placed on the plastic container. The rectifier voltage was regulated based on the target voltages and a copper wire was then attached through the already drilled hole in the mild steel and aluminum samples. The whole cross-section of the samples was allowed to suspend on the connecting rods separated at distances of 5 cm, 10 cm, 15 cm, 20 cm, 25 cm, and 30 cm into the NaCl environment. The experiment was performed on each sample for a duration of 5 min, 10 min, and 15 min under varying voltages of 3 V, 4 V and 5 V for the already specified distances. Subsequently, the anodic and cathodic currents obtained were recorded.

### 2.3.3 Gravimetric (Weight Loss) Measurement

Gravimetric analysis was carried out according to ASTM G103 (2017) standard. The already polished rectangular-shaped mild steel test samples were used. The samples were cleansed with distilled water and dried before being weighed using digital electronic weighing balance with four decimal place accuracy. This was followed by suspension of samples in 400 ml of 0.5 M NaCl solutions contained in three separate beakers. Every 5 days, each test sample was removed from the solution, cleaned with distilled water, dried with a clean towel, and weighed again. Equations (1 and 2) were used to determine the weight loss and corrosion rate, respectively.

$$\text{Weight loss } (\Delta W) = \Delta W_1(\text{Initial weight}) - \Delta W_2(\text{Final weight}) \quad (1)$$

**Table 3** Analytical equipment for study

| Equipment/apparatus | Location |
|---|---|
| Weighing balance | Corrosion Laboratory, Department of Metallurgical and Materials Engineering, FUTA |
| Beakers | Corrosion Laboratory, Department of Metallurgical and Materials Engineering, FUTA |
| Measuring cylinders | Corrosion Laboratory, Department of Metallurgical and Materials Engineering, FUTA |
| Volumetric flask | Corrosion Laboratory, Department of Metallurgical and Materials Engineering FUTA, |
| Potentiostat | Corrosion Laboratory, Department of Metallurgical and Materials Engineering, FUTA |
| Rectifier | Corrosion Laboratory, Department of Metallurgical and Materials Engineering, FUTA |
| Multimeter | Corrosion Laboratory, Department of Metallurgical and Materials Engineering, FUTA |

$$\text{Corrosion Rate(CR)} = \frac{\Delta W \times 87.6}{DAT} \quad (2)$$

where $D$ = density of mild steel in g/cm$^3$. $A$ = total surface area in cm$^2$. $T$ = immersion time in days.

#### 2.3.4 Electrochemical Measurements

Potentiodynamic studies and polarization measurements were performed in compliance with ASTM G3-14 (2014). A computer attached with potentiostat instrument and VERSASTAT-4 was used for this study. NOVA electrochemical software and a three-electrode setup including a counter electrode (graphite electrode), reference electrode (copper rod), and the polished mild steel sample as the working electrode (WE) were used to perform the electrochemical measurement. The working electrode was mounted in epoxy resin and the polished surface was exposed to the environment. The samples were immersed in the environment for a sufficient amount of time to allow for steady state corrosion. At a scan rate of 1 mV/s, potentiodynamic polarization was recorded. The polarization scan's structure was used to anticipate the corrosion behavior, and the relationship between voltage and current as well as the difference between the forward and reverse portions of the scan's relationship were used to interpret the results.

#### 2.3.5 Microstructural Analysis

**2.3.5.1 X-Ray Diffraction Analysis** The corroded (unpolished) samples were collected and prepared for this analysis. A portion of the corroded samples was pelletized and sieved to a size of 0.074 mm. They were then arranged in a 35 × 50 mm aluminum alloy grid on a flat glass plate that was covered with paper. With the use of the Rigaku D/Max-llC X-ray diffractometer, which was developed by the Rigaku Int. Corp. in Tokyo, Japan, the powdery samples were compressed and examined. The device was set up to generate diffractions using a Cu–Kα radiation at a scanning rate of 2°/min in the 2 to 50° range at room temperature. At 40 kV and 20 mA, the diffraction patterns were obtained by applying a $2\theta$ scan range of 10 to 90°, with a step size of 10°. The diffraction data (d value and relative intensity) obtained were compared to that of the standard data of minerals from the mineral powder diffraction file, ICDD which contained and include the standard data of more than 3000 minerals.

**2.3.5.2 Scanning Electron Microscopy/Energy Dispersive Spectroscopy (EDS) Analysis** An Energy dispersive spectroscopy was attached to a scanning electron microscope (SEM) for the analysis of the microstructures. Scanning Electron Microscope (Model: JEOL JSM-6480LV) was used for this analysis. The samples were securely affixed to stubs with the aid of silver paste. To heighten the conductivity of the composite specimens, a slender layer of platinum was subjected to vacuum evaporation onto the surface before photomicrographs were captured at a voltage of 15 kV. The resulting SEM micrographs have a large depth field, giving them a characteristic three-dimensional appearance that is helpful in comprehending a sample's surface structure.

**2.3.5.3 Optical Electron Microscopy** The mild steel samples (unpolished) were analyzed using optical electron microscopy. The electron gun generates electrons. Two sets of condenser lenses focus the electron beam on the specimen and then into a thin tight beam. To move electrons down the column, an accelerating voltage (mostly between 100 and 1000 kV) is applied between tungsten filament and anode. Ultra-thin sections of the samples about 20–100 nm are cut which is already placed on the specimen holder. The electronic beam passes through the specimen and electrons are scattered depending upon the thickness or refractive index of different parts of the specimen. In this microscopy, the denser regions in the specimen scatter more electrons and, therefore, appear darker in the image since fewer electrons strike that area of the screen. In contrast, transparent regions are brighter and the electron beam coming out of the specimen passes to the objective lens, which has high power and forms the intermediate magnified image. The ocular lenses then produce the final further magnified image.

## 3 Results and Discussion

### 3.1 Corrosion Rate of Mild Steel in 0.5 M NaCl Environment

Figure 1 shows the corrosion rate of three samples of mild steel (A, B and C) which were exposed in a 0.5 M NaCl environment for 30 days. It is observed that the corrosion rate of the samples decreased as the exposure time in days increases, which could be as a result of the decrease in the amount of chloride ion which was consumed with increase in exposure time. This agrees with the findings of Sundjono et al. [29] and Elfergani and Abdalla [30] also concluded that corrosion rate of a mild steel increases with increasing chloride ion concentration. It is important to note that chloride ions are responsible for the corrosion of the mild steel. This is because chloride ions have the potential to significantly increase the acidity, resulting in a lower pH of the electrolyte that envelops the steel surface. The heightened acidity facilitates the disintegration of the protective oxide layer, specifically iron oxide, which is naturally present on the surface of the steel. This process exposes the mild steel to more corrosion. Moreover, the interaction between chloride ions and water molecules might result in the formation

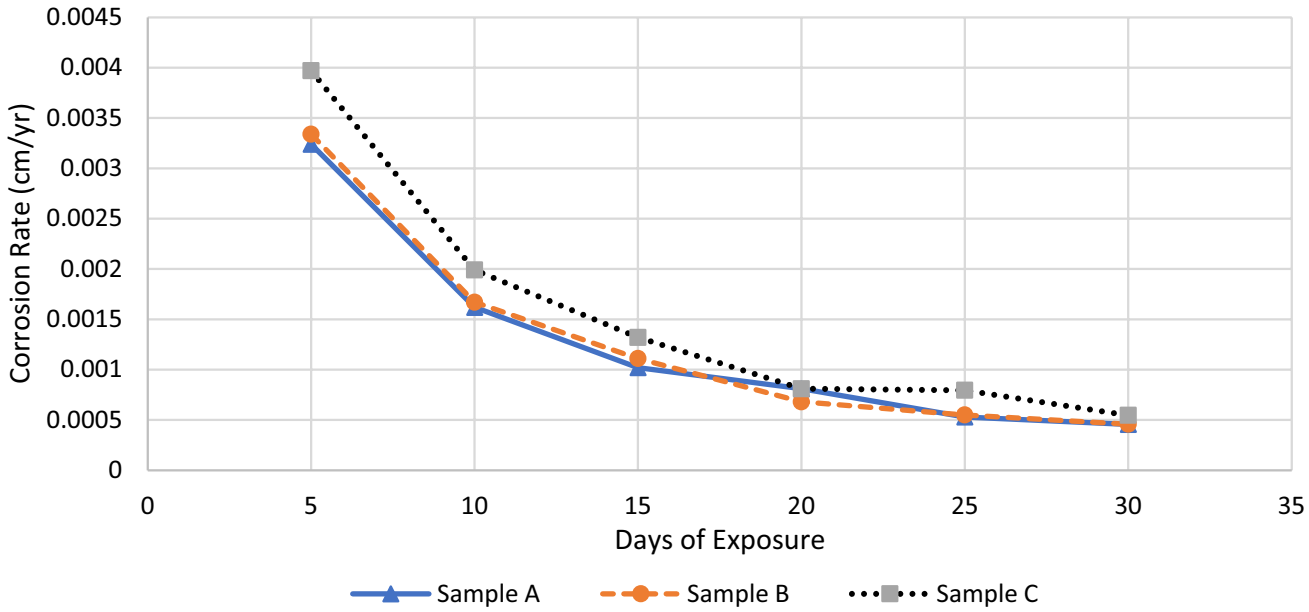


**Fig. 1** Corrosion rate (cm/yr.) against exposure time in days of mild steel in 0.5 M NaCl environment

of hydrochloric acid (HCl), hence expediting the corrosion mechanism. Additionally, chloride ions interfere with the formation and stability of this passive layer. They can disrupt the oxide film by breaking chemical bonds and promoting its dissolution, leaving the steel vulnerable to corrosion attack. The reduction of corrosion rate may also occur due to the pickling occurrence of polished samples that were dipped into the chloride environment. The presence of chloride ions accelerates the corrosion rate of mild steel, this is because chloride ions enhance the electrochemical reactions involved in corrosion, facilitating the dissolution of iron ions from the steel surface and the formation of corrosion in chloride forms such as iron chloride compounds. Additionally, these chloride forms adhere to the surface of the mild steel sample and pickling helps to dissolve these particles which caused a high reduction in the weight of the cathode for the first 5 days as shown in Fig. 1. However, the chemical reactivity of a carbon steel surface immersed in solutions with a substantial amount of chloride ions will likely not be reduced by applying a coating [31].

### 3.2 Physical and Morphological Features

Figure 2a shows physical features of the mild steel samples before immersion in 0.5 M NaCl while Fig. 2b shows one of the mild steel samples after it had been immersed in 0.5 M NaCl environment for 30 days. It was observed that the sample has been attacked by $Cl^-$ ions reducing its shape but not changing its physical structure. Furthermore, from Fig. 2, brownish covering and spots around the sample could be noticed indicating corrosion has occurred on the sample.

Figure 3a–c represents the morphological features; SEM image, EDS spectrum which shows the chemical composition, and the XRD pattern of the corroded (unpolished) mild steel sample, respectively. The SEM micrograph in Fig. 3a showed a possible iron oxide layer arranged in a regular pattern. Thus, indicating the corrosion site of the mild steel which was also confirmed from the EDS spectrum in Fig. 3b. The EDS spectrum displayed optimum peak of iron and also a peak of oxygen which indicates that chloride ions attacked the mild steel after immersion into the NaCl environment causing the formation of oxide forms of iron [iron (III) oxide], which can be described as corrosion. The XRD pattern in Fig. 3c showed possible presence of dual phase of ferrite and pearlite that caused the formation of the anodic and cathodic sites, which may aid corrosion in 0.5 M NaCl environment (which was also confirmed by Ochoa et al. [32]. Additionally, the XRD diffractogram indicated several peaks of iron alloy including the major content of iron which was found at the main peak which appeared between $2\Theta = 35°$ and $2\Theta = 40°$.

Meanwhile, Fig. 4a–c illustrates the relationship between sample A, B, and C, its weight loss and distance. This indicates that each mild steel sample lost weight with an increased rate when the exposure duration is increased. This corroborates the fact that corrosion is occurring, and mild steel samples are being attacked by chloride ion leading to reduction in weight. It is important to note that this characterization was carried out in three samples to ensure the effectiveness of the result.

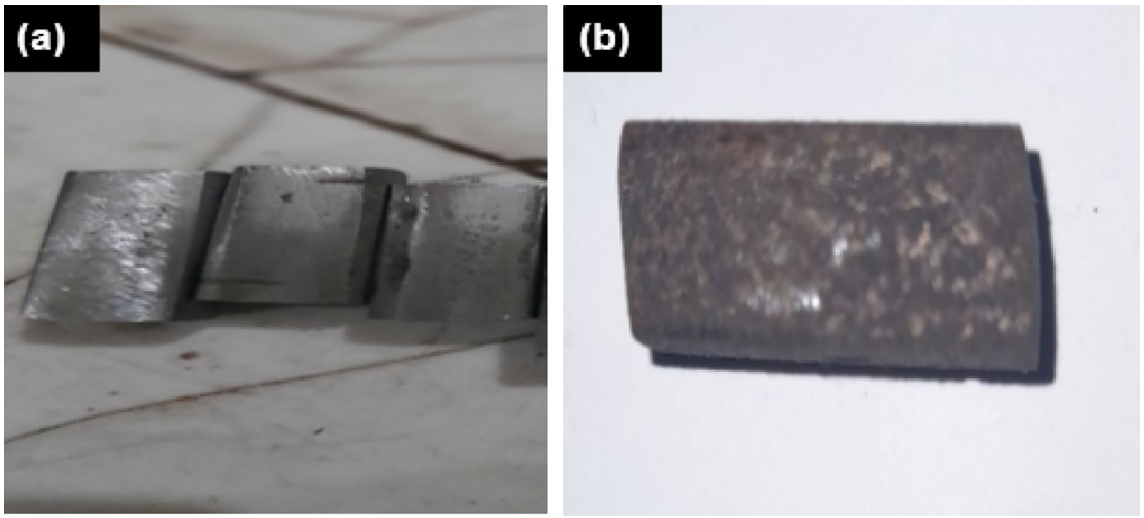


**Fig. 2** **a** Mild steel samples before corrosion in 0.5 M NaCl environment, **b** Mild steel samples after corrosion in 0.5 M NaCl environment

### 3.3 Cathodic Protection Analysis

The graph of corrosion rate against voltage drop is shown in Fig. 5. It was observed that the corrosion rate of the cathode is higher compared to that of the anode, this means that the aluminum anode being a self-passivated metal has been aided by an impressed current system to release electrons from its surface and this could cause the increase in the corrosion rate of the aluminum anode (similar results were reported by Loto et al. [33]). This was also confirmed by the OEM result in Fig. 6a which showed roughly dispersed aluminum particles on the cathode surface. Thus, the mild steel cathode is being protected by the deposited aluminum due to the impressed current system which suppressed the self-passivated properties of aluminum. In addition, the SEM result in Fig. 6b gives a higher magnification of almost spherical aluminum particles, roughly dispersed with relatively broad particle size distributions on the surface of the cathode. While no peaks of aluminum were found on the surface of the initial mild steel sample prior to cathodic protection in a 0.5 M NaCl environment, as indicated by the EDS and XRD results presented in Fig. 3b and c, respectively, the XRD result in Fig. 6d demonstrated the presence of aluminum and its compounds on the surface of the mild steel sample. However, after cathodic protection, the presence of aluminum and its compounds was shown by the XRD result in Fig. 6d. This result was supported by the EDS elemental analysis result presented in Fig. 6c. These results corroborate the fact that the aluminum anode undergoes corrosion in preference to the cathode (mild steel) sample. As stated by Loto et al. [33], the anode provides current while progressively dissolving into ions in the environment employed. During cathodic protection, the anode is more active than the cathode. The cathode obtains electrons from the anode through their metallic connection at the same time that the anode produces electrons. As a result, the cathode is protected from corrosion and becomes negatively polarized.

### 3.4 Potentiodynamic Polarization Analysis

The potentiodynamic polarization pattern of aluminum and mild steel, which were utilized as the cathode and anode, respectively, is shown in Fig. 7. It was observed clearly from the graph that the aluminum anode sample had more electronegative potential of − 1 V than the cathode sample (mild steel) which was a bit closer to − 0.8 V. This means that the aluminum anode can sacrificially protect the mild steel and will readily release electrons from its surface to protect the mild steel from corrosion, thus corroding in preference to the cathode. Consequently, there will be no passivity (the formation of oxide layer on the surface of the material) which will cause the anode to be protected in preference to the cathode [15].

Furthermore, from Fig. 7 the current density of aluminum anode ($1.00 \times 10^{-5}$ A/cm$^2$) was observed to be slightly higher than the mild steel cathode ($1.54 \times 10^{-6}$ A/cm$^2$), thus confirming that the rate of corrosion will be more in the anode than the cathode which has a lower value of the current density. Increased current is an indication of increasing corrosion rate [33].

### 3.5 Voltage Drop with a Varying Distance Measurement

From Fig. 8, it could be observed that voltage drop increases as cathode–anode distance increases for 3 V, 4 V, and 5 V. An increase in the cathode–anode distance could result in a reduction in the driving force needed to

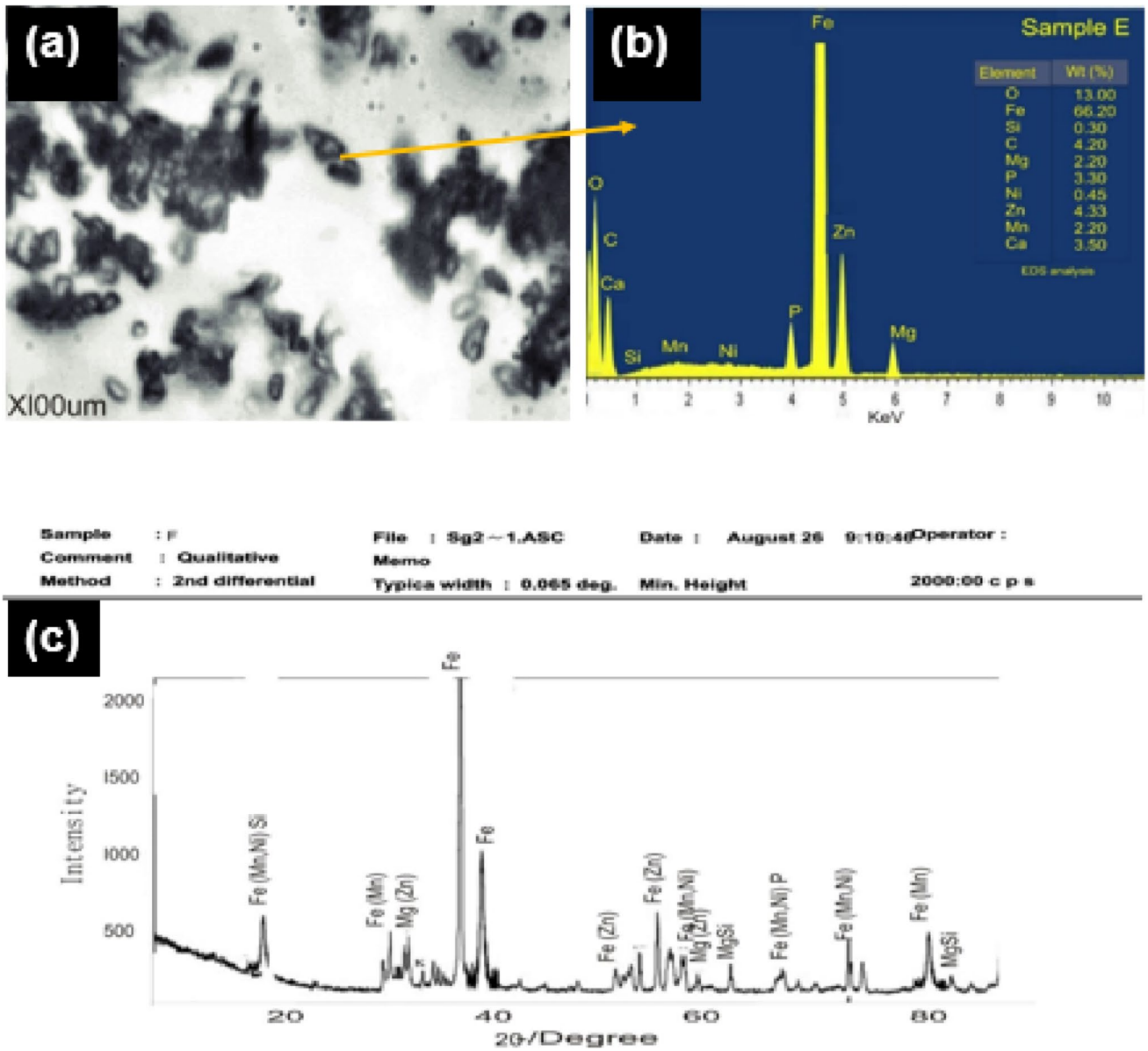


**Fig. 3** **a** SEM micrograph, **b** EDS and **c** XRD pattern of the corroded mild steel sample

drive the electrons from the anode (aluminum) to cathode (mild steel) and as well reduce the tendency for protection likeliness of cathode by the anode. In this study, it is evident that the corrosion rate decreases, and voltage drop increases in presence of cathodic protection. These findings corroborate those of Brenna et al. (2013), who found that cathode–anode distance is one of the factors influencing corrosion rate—that is, a shorter distance corresponds to a higher rate of corrosion. This outcome can also be explained by the fact that the HCl electrolyte is becoming more resistant, which implies that as the distance between the anode and cathode increases, the electrolyte's conductivity will decrease. Accordingly, as the solution's resistance increases, the cathodic protection current density rises [34].

## 3.6 Cathode Weight Measurement with Varying Distance, Time, and Rectifier Voltage

### 3.6.1 Cathode Weight Measurement with a Voltage of 3 V

With the application of 3 V from the rectifier and a cathode–anode distance of 5 cm, it was observed from Fig. 9 that the cathode weight increases from 0.001 to 0.003 as the exposure time progressed from 5 to 15 min. Also, at a distance of 10 cm there was a constant weight of cathode

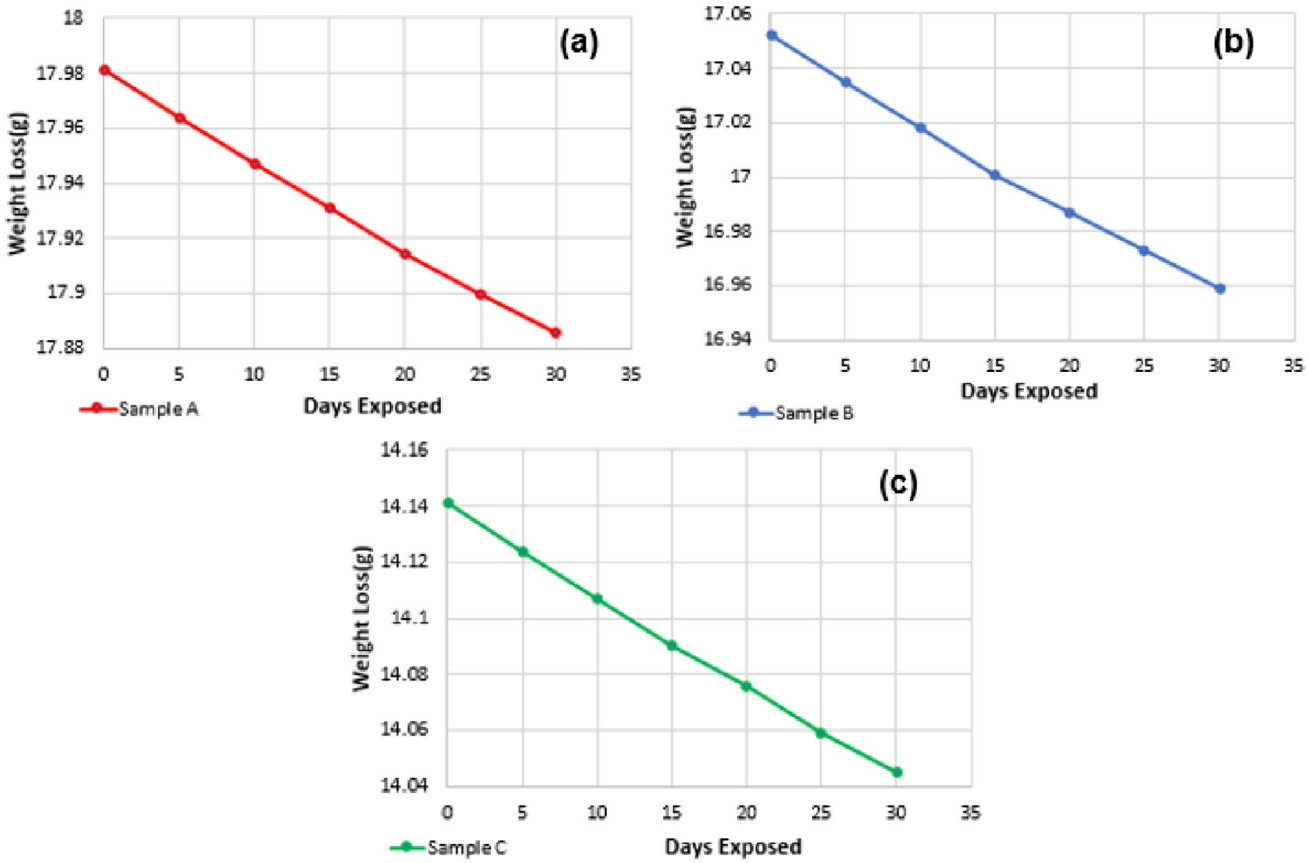


**Fig. 4** Weight loss over 30 days exposure time **A** sample A, **B** sample B and **C** sample C, immerse in 0.5 M NaCl environment

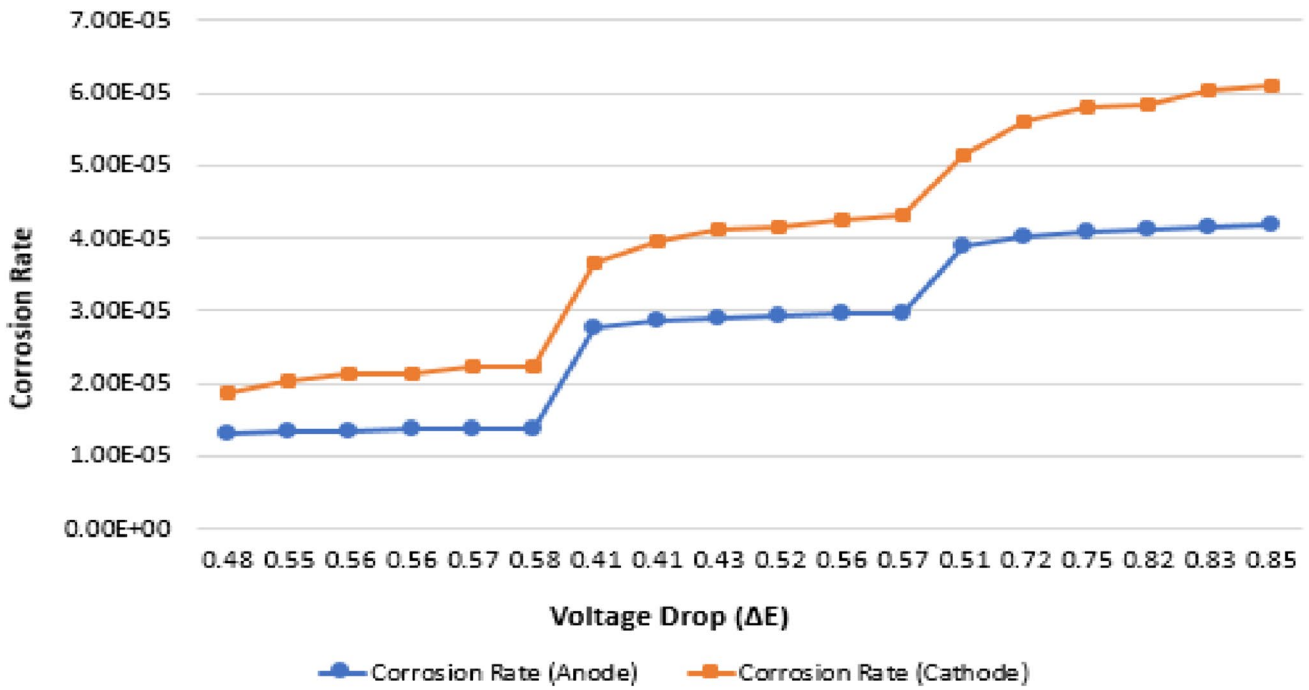


**Fig. 5** Corrosion rate against voltage drop (ΔE) in 0.5 M NaCl environment

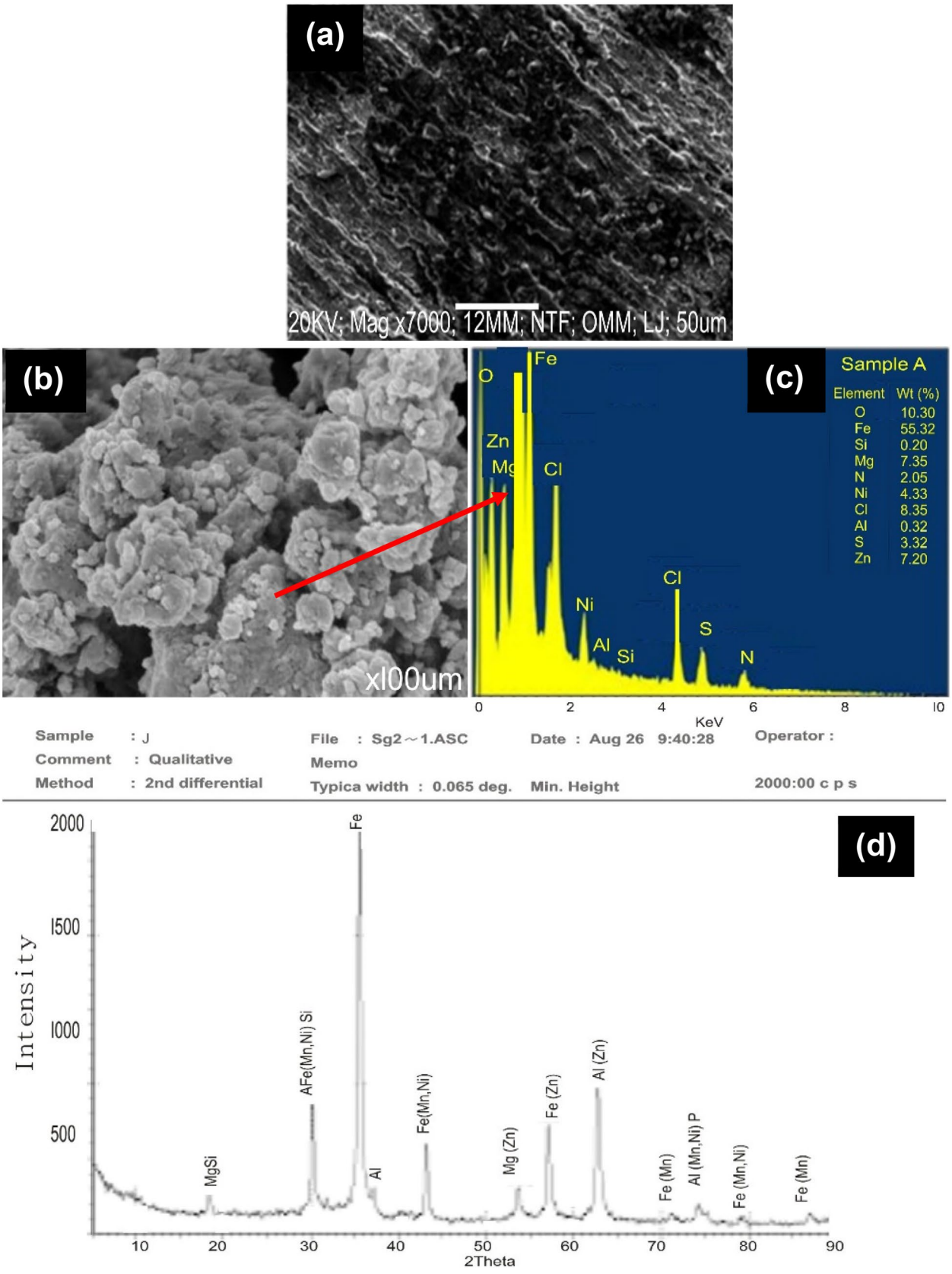


**Fig. 6** **a** OEM image, **b** SEM micrograph, **c** EDS spectrum, **d** XRD pattern of the mild steel sample after cathodic protection in 0.5 M NaCl environment

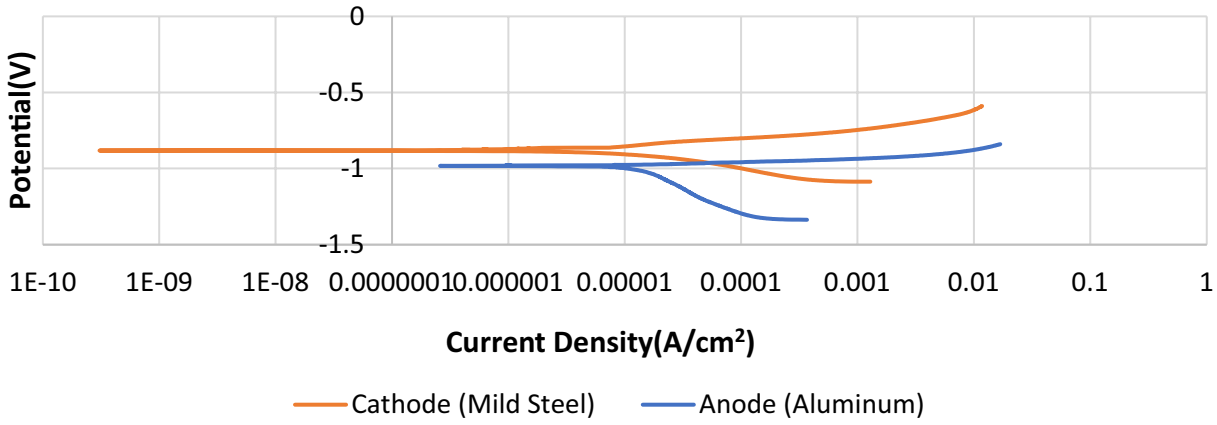


**Fig. 7** Potentiodynamic polarization (Tafel Plot) in 0.5 M NaCl environment

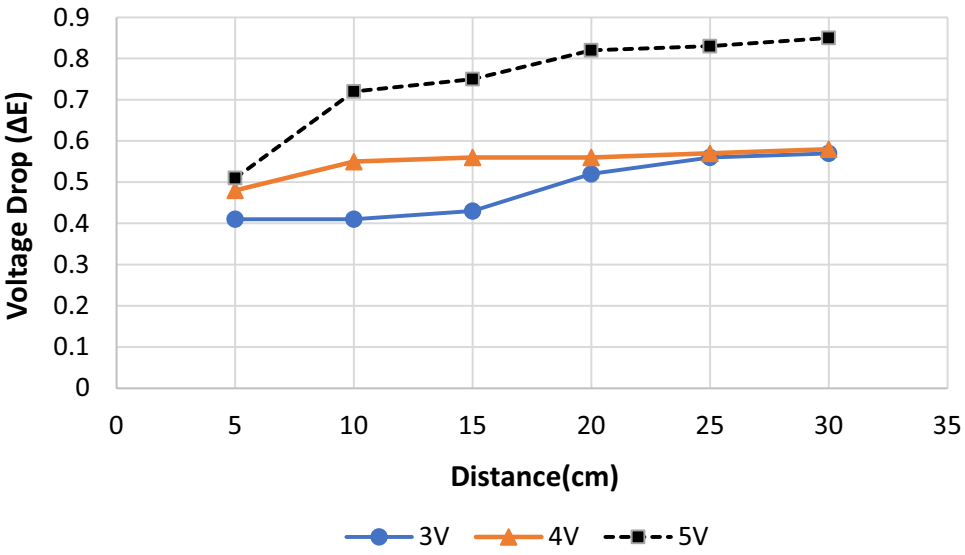


**Fig. 8** Voltage Drop (ΔE) against distance in 0.5 M NaCl environment

of 0.001 at a rate of 5 to 10 min, and a decrease in weight of 0.002 at 10 min when compared with the distance of 5 cm. Hence, it can be deduced that the weight of cathode decreases with increase in distance for a period of 5 to 15 min, which could be as a result of the amount of aluminum deposited on the cathode at a shorter distance as investigated by Nayebi and Ayati, [35]. The authors concluded that the distance between the electrodes cannot be underestimated. In this work, it was observed that reducing the distance between the anode and cathode lead to an appreciable increase in the amount of disposition of aluminum electrons on the cathode, which results in more protection of the cathode by the anode. Consequently, this yields a reduction in the corrosion rate of the protected cathode. The observed phenomenon can also be attributed to the decreasing conductivity of the electrolyte with increasing cathode–anode distance. According to Lacroix et al. [36], cathodic protection increased with an increasing electrolyte resistance. This result depicts that given a chemical composition shown in Tables 1 and 2, for a cathode sample (mild steel) with a cross sectional area of 10.26 $cm^2$ and aluminum sample with cross-sectional area of 15.82 $cm^2$, respectively, the cathode (mild steel) sample will be cathodically protected by aluminum ion deposited on its surface at 3 V in 0.5 M NaCl environment.

### 3.6.2 Cathode Weight Measurement with a Voltage of 4 V

From the graph in Fig. 10, with the application of 4 V from the rectifier it could be seen that the weight of the cathode increased from 0.001 to 0.005 at a cathode–anode distance of 5 cm as the time moved from 5 to 15 min. The increase in weight was more compared to the observed weight increase under a voltage of 3 V from the rectifier

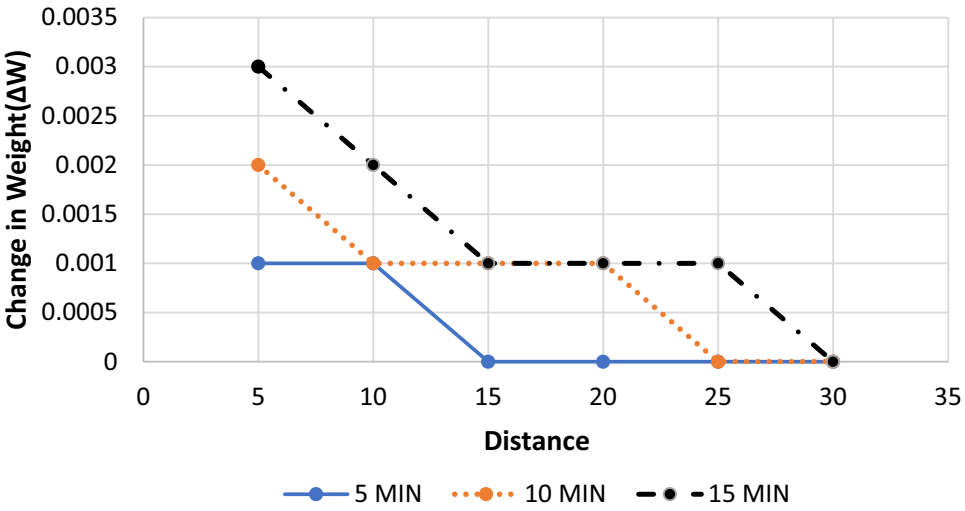


**Fig. 9** Weight of cathode against Anode–Cathode distance (Cm) at 3 V In 0.5 m NaCl environment

for 15 min. This further corroborated the fact that the more aluminum deposition on the cathode, the higher the cathode weight, and the more the tendency for the cathode to be protected against corrosion. Moreover, as the cathode–anode distance increases, the weight of the cathode decreases. With this finding, the amount of deposition on the cathode was observed to be higher with increase in the voltage from 3 to 4 V supplied from the rectifier, consequently the cathode (mild steel) sample with a cross sectional area of 10.26 $cm^2$ and chemical composition shown in Table 1 will be cathodically protected efficiently at 4 V in 0.5 M NaCl environment. Moreover, 4 V from the rectifier will be sufficient to overcome passivation and drive the electrons sporadically from the aluminum–anode to the surface of the mild steel-cathode.

#### 3.6.3 Cathode Weight Measurement with a Voltage of 5 V

With an application of 5 V from the rectifier, the cathode weight decreases at a cathode–anode distance of 5–15 cm as time increases from 5 to 15 min (Fig. 11). The increase in cathode weight here cannot be undermined but, in this case, the weight increment of the cathode only occurred only for 5 min at 30 cm and became neutral at 20 cm and 25 cm for the same 5 min duration. This shows that the cathode sample was only protected at 20 cm, 25 cm and 30 cm for 5 min. It also shows that at 5 V from the rectifier and distances of 5 cm, 10 cm, 15 cm, the cathodic sample was over protected and could cause cathodic disbondment to occur. Cathodic disbondment can arise in a situation where the cathodic coating loses its adhesion to the steel due to the voltage originated from cathodic protection [37]. Conclusively, this shows that a cathode (mild steel) sample of cross-sectional area of 10.26 $cm^2$ will be cathodically protected by aluminum anode at 5 V only with distances of 20 cm, 25 cm, 30 cm for 5 min in 0.5 M NaCl environment.

### 3.7 Measurement of Aluminum Deposited at the Cathode with Varying Voltage and Distance

Figure 12 shows the amount of aluminum deposited at the cathode with varying voltages of 3 V, 4 V, and 5 V supplied from the rectifier and with varying cathode–anode

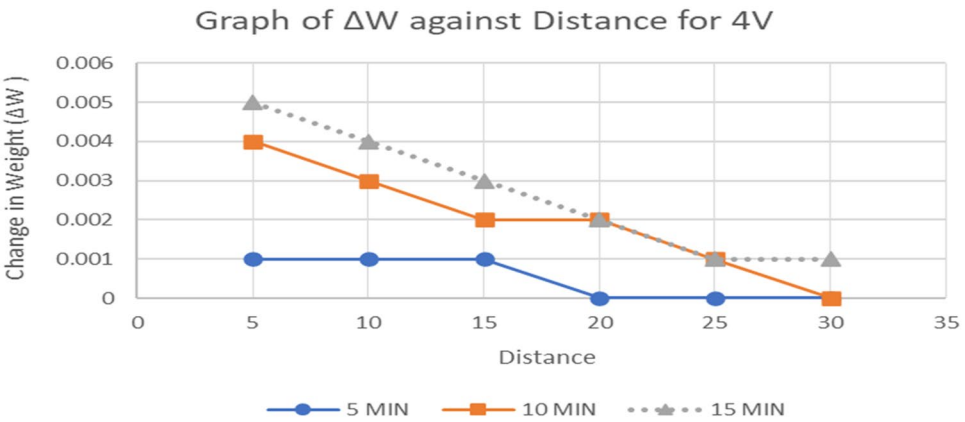


**Fig. 10** Change in weight against anode–cathode distance (cm) at 4 V in 0.5 M NaCl environment

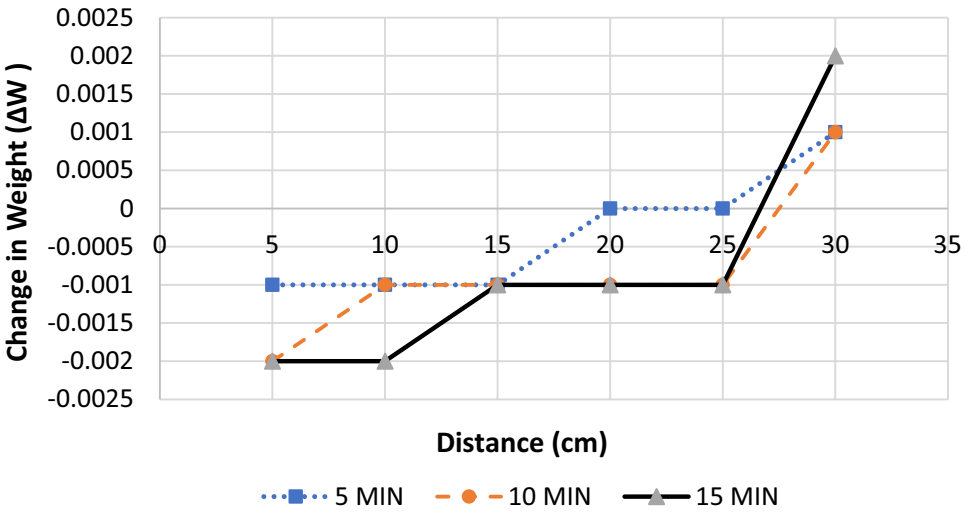


**Fig. 11** Change in weight against distance (cm) at 5 V in 0.5 M NaCl environment

distances of 5 to 30 cm. It could be observed that as the voltage increased for all the setups with a cathode–anode distance of 5 cm, the amount of aluminum deposited at the cathode also increased. Although this was not applicable all through for the varying distance and voltage, this could be a result of the increment in distance for the cathode sample in which 5 V was supplied which led to the drastic reduction in the amount of aluminum deposition at 25 cm, 20 cm, 15 cm, 10 cm, 5 cm for 5 V. This could be because the system started giving reverse protection at 5 V and the anode became the cathode, this made the anode get protected by the cathode instead of the cathode getting protected by the anode. The reversed protection was triggered due to the increase in corrosion rate at that particular stage which led to the corrosion of the cathodic mild steel as depicted by the graph in Fig. 12. The cathodic sample became over-protected at 5 V and a distance of 10 cm. Fitrullah et al. [37] confirmed that the over-protection may have caused a cathodic disbandment, in which the cathodic coating loses its adherence to the steel as a result of the voltage arising from cathodic protection. This further corroborates the results in Fig. 11 that a cathode (mild steel) sample with a cross-sectional area of 10.26 $cm^2$ will be cathodically protected efficiently by an aluminum anode at 5 V only at distances of 20 cm, 25 cm, and 30 cm in 0.5 M NaCl environment.

### 3.8 Change in Weight Measurement for Cathode and Anode at 3v

With a rectifier voltage of 3 V and distance of 5 cm which could be suitable for cathode–anode distance in a cathodic protection experiment according to Figs. 9 and 10 and from Table 3, it could be observed that the amount of anode needed to achieve protection of 0.003 g was 0.007 g of the anode. However, the amount of mass leaving the anode should be equal to the amount of mass deposited on the surface of the cathode, which is not so according to Table 4, and this is against the law of conservation of matter. This could be because the full deposition of aluminum electrons on the cathode mild steel was reduced due to the loss of certain

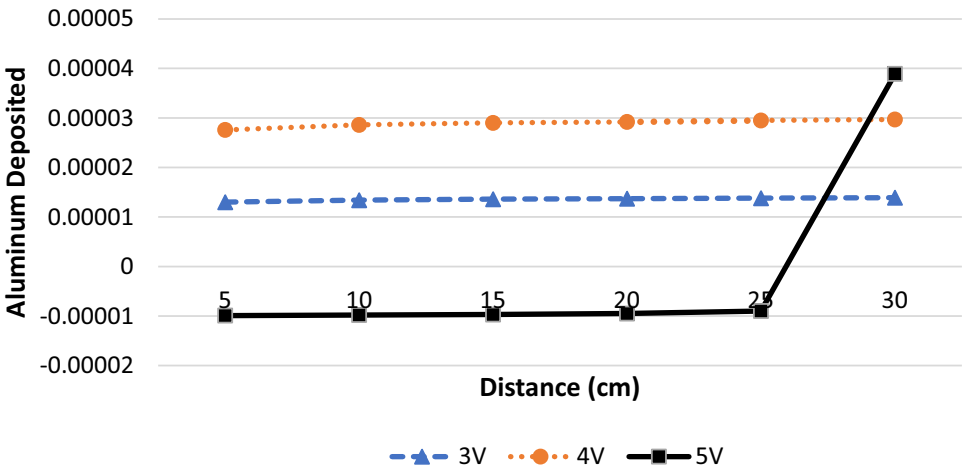


**Fig. 12** Amount of aluminum deposited at cathode against distance (cm) in 0.5 M NaCl environment

**Table 4** Change in weight values for cathode and anode at 3 V in 0.5 M NaCl environment

| Distance (cm) | ΔW1 (Cathode) | ΔW2 (Cathode) | ΔW3 (Cathode) | ΔW1 (Anode) | ΔW2 (Anode) | ΔW3 (Anode) |
|---|---|---|---|---|---|---|
| 5 | 0.001 | 0.002 | 0.003 | − 0.002 | − 0.002 | − 0.007 |
| 10 | 0.001 | 0.001 | 0.002 | − 0.019 | − 0.031 | − 0.043 |
| 15 | 0 | 0.001 | 0.001 | − 0.016 | − 0.014 | − 0.012 |
| 20 | 0 | 0.001 | 0.001 | − 0.019 | − 0.009 | − 0.01 |
| 25 | 0 | 0 | 0.001 | − 0.01 | − 0.013 | − 0.03 |
| 30 | 0 | 0 | 0 | − 0.014 | − 0.026 | − 0.037 |

metallic ions from the aluminum in the electrolyte. The lost metallic ions in the electrolyte could cause the cathode to be neutral and not protected because the solution (electrolyte) has been fully saturated with enough metallic ions. Thus, the metallic ions released from the anode will be attacked by the chloride ions of the corrosive medium (0.5 M NaCl).

## 4 Conclusions

In this work, the outcome of varying cathode–anode parameters on performance of mild steel cathodically protected by the aluminum anode in 0.5 M NaCl environment was successfully investigated. The cogent findings of this work are summarized as follows:

- The corrosion rate of the three samples of mild steel (A, B and C) exposed for 30 days in 0.5 M NaCl environment decreases as the exposure time in days increases.
- In a 0.5 M NaCl environment, aluminum anodes sacrificially protect the mild steel cathode. However, they only do so for a short while before passivating or forming an oxide layer on the anode's surface. To de-passivate the aluminum anode and provide the mild steel cathode with cathodic protection, an impressed current system is needed.
- The mild steel cathode was cathodically protected by the aluminum anode at 3 V in 0.5 M NaCl environment across the cathode–anode distances studied in this work. However, the cathode (mild steel) sample was efficiently protected by the sacrificial aluminum anode at 4 V in 0.5 M NaCl environment for distances of 5 cm for 15 min. In addition, a rectifier voltage of 4 V was found to be the most suitable voltage to overcome passivation and ensure deposition of the electrons from the aluminum anode on the surface of the cathode (mild steel).
- Furthermore, in 0.5 M NaCl environment and a rectifier voltage of 5 V, the cathode was efficiently protected at cathode–anode distances of 20 cm, 25 cm, 30 cm for 5 min, while cathodic disbondment due to the overprotection of the cathode was observed at lower cathode–anode distances ranging between 5 and 15 cm. Therefore, variance in time, distance, and voltage is crucial to the aluminum anode's ability to effectively provide cathodic protection.

In summary, effective corrosion protection was established by employing aluminum as an anode for cathodic protection of mild steel in a 0.5 M NaCl environment. A continuous supply of electrons was effectively provided by the aluminum anode to the mild steel cathode, resulting in the mitigation of corrosion and prevention of the degradation of mild steel. Several characteristics, such as the distance between the anode and cathode, the surface area ratio of the anode to the cathode, and the applied current density, exerted an influence on the performance of the cathodic protection system. The identification of ideal settings that maximized corrosion protection while minimizing energy consumption and system complexity was achieved through a series of experiments. The performance of the cathodic protection system was significantly influenced by the distance between the anode and cathode. The increased closeness between the anode and cathode led to improved electron transfer efficiency and heightened corrosion resistance. The results obtained from this experiment hold significant practical significance for the development and enhancement of cathodic protection systems implemented in mild steel structures situated in settings with high chloride concentrations like the maritime industry and sub-sea operations. Engineers and scientists can optimize cathodic protection systems for structural applications by comprehending the impact of cathode–anode characteristics on system performance. This enables effective mitigation of corrosion and maintain long-term structural integrity.

**Acknowledgements** Department of Mechanical Engineering, Redeemer's University, Nigeria. Department of Metallurgical and Materials Engineering, Federal University of Technology, Akure, Nigeria.

**Author Contributions** This work was carried out in collaboration between all authors. Daniel Toyin Oloruntoba, Temitope Ebenezer Odemona, and Williams Temitope Owolabi designed the study, performed the experiment, interpreted results and wrote the first draft of the manuscript. Authors, Olanrewaju Seun Adesina, Olufemi Oluseun Sanyaolu, & Azeez Lawan Rominiyi managed the analyses of the study,

managed literature searches and graphical editing. All authors read and approved the final manuscript.

**Funding** The authors received no funding from any source.

**Data Availability** All data employed in support to the outcome of the study are included in this article.

## Declarations

**Competing Interests** The authors declare no competing interest with any previous work.

## References


1. Saha MK, Das S (2016) A review on different cladding techniques employed to resist corrosion. J Assoc Eng 86(1–2):51–63
2. Otunniyi IO, Oloruntoba DT (2012) Suitability of structural aluminium profiles as sacrificial anode for carbon steel. Leonardo Electron J Pract Technol 21:62–72
3. Hajar HM, Suriani MJ, Sabri MGM, Ghazali MJ, Nik WW (2015) Corrosion performance of coating thickness in marine environment. Biosci Biotechnol Res Asia 12(1):71–76
4. Usher KM, Kaksonen AH, Cole I, Marney D (2014) Critical review: microbially influenced corrosion of buried carbon steel pipes. Int Biodeterior Biodegrad 93:84–106
5. Kumar A (2015) Corrosion behavior of low carbon steel in presence of chlorides, cyanides, and sulphates (Doctoral dissertation)
6. Biesuz M, Pinter L, Saunders T, Reece M, Binner J, Sglavo VM, Grasso S (2018) Investigation of electrochemical, optical and thermal effects during flash sintering of 8YSZ. Materials 11(7):1214
7. May M (2016) Corrosion behavior of mild steel immersed in different concentrations of NaCl solutions. J Sebha Univ 15(1):1
8. Angst U, Büchler M, Martin B, Schöneich HG, Haynes G, Leeds S, Kajiyama F (2016) Cathodic protection of soil buried steel pipelines—a critical discussion of protection criteria and threshold values. Mater Corros 67(11):1135–1142
9. Liu Y, Song Z, Wang W, Jiang L, Zhang Y, Guo M, Xu N (2019) Effect of ginger extract as green inhibitor on chloride-induced corrosion of carbon steel in simulated concrete pore solutions. J Clean Prod 214:298–307
10. Wilson K, Jawed M, Ngala V (2013) The selection and use of cathodic protection systems for the repair of reinforced concrete structures. Constr Build Mater 39:19–25
11. Xu L, Xin Y, Ma L, Zhang H, Lin Z, Li X (2021) Challenges and solutions of cathodic protection for marine ships. Corros Commun 2:33–40
12. Bagastyo AY, Anggrainy AD, Khoiruddin K, Ursada R, Warmadewanthi IDAA, Wenten IG (2022) Electrochemically driven struvite recovery: prospect and challenges for the application of magnesium sacrificial anode. Sep Purif Technol 288:120653
13. Ding Q, Shen T, Cui Y, Xue J (2018) Study on the electrochemical performance of sacrificial anode interfered by DC stray current. Int J Corros. https://doi.org/10.1155/2018/4728692
14. Gordon DF (2018) Hydrogen re-embrittlement susceptibility of ultra high-strength steels. Ph.D. Thesis, Cranfield University, School
15. Silva Campos MDR, Blawert C, Scharnagl N, Störmer M, Zheludkevich ML (2022) Cathodic protection of mild steel using aluminium-based alloys. Materials 15(4):1301
16. Shreir LL (1994) Corrosion: corrosion control, 2nd edn. Butterworths, London
17. Baboian R (2005) Corrosion tests and standards: application and interpretation, 2nd edn. ASTM International, Baltimore
18. Shreir LL (1965) Corrosion: metal/environment reactions, 2nd edn. Newnes-Butterworths, London
19. Occupational Safety and Health Administration. 1910.1027—Cadmium|occupational safety and health administration. Available online: https://osha.gov (Accessed, March 2022).
20. Holm O, Hansen E, Lassen C, Stuer-Lauridsen F, Kjolholt J (2002) Heavy metals in waste final report DG ENV. E3, Project ENV. E; European Commission, Brussels
21. Loto CA, Popoola API (2011) Effect of anode and size variations on the cathodic protection of mild steel in sea water and sulphuric acid
22. Frankel G (2015) WR Whitney award lecture: the effects of microstructure and composition on Al alloy corrosion. Corrosion 71:1308–1320
23. Baker D, Druschitz A (2016) Understanding the corrosion of low-voltage Al–Ga anodes. In: Proceedings of the corrosion, Vancouver, BC, Canada, 6–10 March 2016.
24. Feng X, Yan Q, Lu X, Wu T, Zhang Y, Zuo Y, Wang J (2020) Protection performance of the submerged sacrificial anode on the steel reinforcement in the conductive carbon fiber mortar column in splash zones of marine environments. Corros Sci 174:108818
25. Schuman TP (2018) Protective coatings for aluminum alloys. Handbook of environmental degradation of materials. William Andrew Publishing, Oxford, pp 423–448
26. Al-Sultani KF, Nabat JN (2012) Effects of tin on Aluminum–Zinc alloy as sacrificial anode to protect underground oil pipeline in Al-Mahawil regional. Adv Mater Res 468:1585–1594
27. Umoru LE, Ige OO (2007) Effects of tin on aluminum–zinc–magnesium alloy as sacrificial anode in seawater. J Miner Mater Charact Eng 7(2):105–113
28. Alzwghaibi AAA, Saeed EM, Klif DF (2011) Cathodic protection of oil pipelines by aluminum alloys. J King Abdulaziz Univ 22(2):17
29. Sundjono S, Priyotomo G, Nuraini L, Prifiharni S (2017) Corrosion behavior of mild steel in seawater from northern coast of Java and southern coast of Bali, Indonesia. Bandung Institute of Technology, Bandung
30. Elfergani HA, Abdalla AA (2017) Effect of chloride concentration on the corrosion rate of carbon steel. In: 2nd Libyan conference on chemistry and its application (LCCA). pp 33–38
31. Nam ND, Van Hien P, Hoai NT, Thu VTH (2018) A study on the mixed corrosion inhibitor with a dominant cathodic inhibitor for mild steel in aqueous chloride solution. J Taiwan Inst Chem Eng 91:556–569
32. Ochoa N, Vega C, Pébère N, Lacaze J, Brito JL (2015) $CO_2$ corrosion resistance of carbon steel in relation with microstructure changes. Mater Chem Phys 156:198–205
33. Loto CA, Loto RT, Popoola PA (2019) Evaluation of cathodic protection of mild steel with magnesium anodes in 0.5 M HCL. Chem Data Collect 22:100246
34. Liu Y, Gao Z, Lu X, Wang L (2019) Effect of temperature on corrosion and cathodic protection of X65 pipeline steel in 3.5% NaCl solution. Int J Electrochem Sci 14(1):150–160
35. Nayebi B, Ayati B (2021) Degradation of emerging amoxicillin compound from water using the electro-Fenton process with an aluminum anode. Water Conserv Sci Eng 6:45–54
36. Lacroix R, Da Silva S, Gaig MV, Rousseau R, Délia ML, Bergel A (2014) Modelling potential/current distribution in microbial electrochemical systems shows how the optimal bioanode architecture depends on electrolyte conductivity. Phys Chem Chem Phys 16(41):22892–22902
37. Fitrullah M, Mawaddah SM, Tarigan P, Soesaptri O, Trenggono A (2016) The effect rust and over-protection voltage of impressed

current cathodic protection towards LR grade a steel disbondment. Appl Mech Mater 842:92–98